Effective temperatures of magnetic CP stars from full spectral energy distributions

Ł. Lipski[1] and K. Stępień[1]

[1] *Warsaw University Observatory, Al. Ujazdowskie 4, 00-478 Warszawa, Poland*

ABSTRACT

New determinations of effective temperatures of 23 magnetic, chemically peculiar (mCP) stars were obtained from a fit of metal enhanced model atmospheres to the observed spectral energy distributions (SED) from UV to red. Temperatures of four more CP stars without magnetic measurements were also obtained, of which three show light variations characteristic of magnetic variables, and the fourth may possibly be normal. The root-mean-square (RMS) method was used to fit the theoretical SED to the observations corrected for reddening if necessary, with metallicity and effective temperature as the fitting parameters. Gravity was assumed to be equal to $\log g = 4$ for main sequence stars and to $\log g = 3$ for two giants in the considered sample. Equal weights were given to the UV part and visual part of SED. An attempt was made to obtain a three-parameter fit (with reddening included) to the observed SED of HD 215441. It turned out that the three-parameter fit gave spurious results due to correlations among the parameters. We could determine the reddening of that star only by *assuming* that the metallicity of the model is known, hence reducing the number of fitting parameters to two.

Independently of the formal quality of fit resulting from the RMS method applied to the whole SED, the quality of fit was additionally checked for each star by determination of the temperature from the best fitting model atmosphere to the UV part and the visual part of SED separately. Both temperatures should be close to one another if the global best fitting model satisfactorily describes the full observed SED. This is the case for about a half of the investigated stars but the difference exceeds 750 K for the remaining stars with the extreme values above 2000 K. Possible reasons for such discrepancies are discussed.

New, revised calibrations of effective temperature and bolometric corrections of mCP stars in terms of reddening free Strömgren indices are given.

Key words: stars: chemically peculiar – stars: fundamental parameters

1 INTRODUCTION

Effective temperature, T_e, is the stellar parameter of crucial astrophysical importance. It needs to be accurately known prior to any detailed analysis of stellar structure and evolution. According to definition, effective temperature is determined from the integrated emergent energy flux which, in turn, can be calculated from the observed energy distribution and angular diameter of the star (Code et al. 1976). The method cannot be used on a massive scale because accurate observations of the energy distribution and angular diameters are available for a limited number of stars only. Such stars serve usually as standards for calibration of other temperature measures of which most useful are color indices observed with different pho-

tometric systems. To avoid problems with measuring angular diameters indirect methods have been suggested, like the infrared flux method (IRFM) in which the diameter can be calculated from the ratio of the observed to (stellar) surface monochromatic flux in infrared, assuming its weak dependence on temperature (Blackwell & Shallis 1977). Since a large grid of realistic model atmospheres computed by Kurucz (1979, 1992) has became available (see http://kurucz.harvard.edu./grids.html) effective temperature of a star can be determined from a fit of a theoretical emergent flux to the observed energy distribution. Model atmospheres are available for a broad range of temperatures, gravities and different metal abundances (scaled solar abundances). With effective temperature known, the angular diameter can be calculated from the total observed

energy flux. Because the energy distribution depends only weakly on surface gravity, the simultaneous determination of temperature and gravity is impractical, even in case of stars with known metallicity. Surface gravity is usually determined from other data, e. g. from Balmer lines or spectral type. On the other hand, energy distributions of two models with the same T_e and $\log g$ but different metal abundances may differ significantly. Metals produce a large number of spectral lines in the UV, which block effectively a noticeable fraction of the flux (this is called blanketing effect). The blocked flux is radiated in longer wavelengths due to backwarming effect (an increase of temperature of the corresponding atmospheric layers). Increased metal abundance modifies the temperature distribution as a function of optical depth in a sense that temperature is higher, compared to normal metal abundance star, in layers where the visual part of the spectrum is formed and it is lower in layers where the UV part of the spectrum is formed. As a result, calibrations based on visual energy distributions of normal stars are not applicable to metal rich stars as they give systematically too high effective temperatures. Stars with chemical composition deviating significantly from solar should be calibrated separately.

Several groups of chemically peculiar (CP) stars with non-solar abundances exist among upper main sequence stars (Preston 1974). One of them is a group of magnetic CP (mCP) stars. They show a presence of strong, ordered surface magnetic fields with intensities up to several kilo-Gauss (Bychkov et al. 2003), associated with large atmospheric overabundances of heavy elements, among them silicon, rare earth elements and iron peak elements (Preston 1974). Compared to other peculiar stars, e. g. HgMn, λ Boo type or Am stars, mCP stars show the largest deviations of spectral energy distribution (SED) from normal stars. The overabundant elements block effectively the UV flux which is re-radiated in longer wavelengths, similarly as in metal rich stars. However, a precise shape of SED of each mCP star depends sensitively on its detailed chemical composition. In many such stars elements are not evenly distributed over the atmosphere. Instead, they show concentrations in some parts of the stellar surface (chemical spots) and are nonuniformly distributed in the vertical direction (Ryabchikova 2003). All this complicates enormously modeling of their atmospheres. Even if one considers only a surface averaged model of mCP star, the correct approach requires an iterative process in which the atmospheric parameters and chemical abundances are corrected at each step. Such a procedure has not been so far applied to mCP stars. Several years ago there have been attempts to model the observed energy distributions of a few stars with individually tailored, but fixed, chemical compositions (Muthsam & Stępień 1980; Stępień & Muthsam 1987) but, due to a shortage of the modeling procedure, significant discrepancies between the observed and computed SED remained. Very few individual SED of chemically peculiar stars have been modeled since then (see http://wwwuser.oat.ts.astro.it/castelli).

Many attempts to determine effective temperatures of mCP stars can be found in literature. Unfortunately, most of them are based on photometry or, at best, on visual parts of SED (Hauck & North 1993; Sokolov 1998; Adelman & Rayle 2000). As a result they are prone to systematic errors arising from peculiar SED and uncertain red-dening corrections. Stępień & Dominiczak (1989) analyzed full SEDs (visual + UV from IUE) but, in lack of metal enhanced models at that time, they fitted the Kurucz solar composition models to the visual parts of SED and then they calculated corrections resulting from the UV flux deficit to obtain final effective temperatures.

On the other hand, a large volume of photometric data in different photometric systems exist for peculiar stars, which could be used to determine their temperatures if reliable calibrations exist for them (Moon & Dworetsky 1985; Hauck & North 1993; Napiwotzki et al. 1993; Hauck & Künzli 1996). A critical analysis of some of them is given by Stępień (1994).

The purpose of the present paper is to determine effective temperatures of mCP stars for which UV and visual scans exist, by fitting metal enhanced model atmospheres to dereddened (if necessary) SED. Thus determined temperatures can be used to improve existing calibrations of photometric color indices. Selection criteria for including a star into our analysis and stellar observational data are described in the next section together with the method of obtaining the final observed SED. The fitting method of model atmospheres to the observations and the results are given in Section 3 together with the discussion and new calibrations in terms of the color indices from Strömgren photometry. The last section summarizes the main conclusions.

2   SELECTION OF STARS AND DATA SOURCES

A star had to fulfill simultaneously the following criteria to be included into further analysis:

- to be classified as chemically peculiar of CP2-type (Preston 1974),
- to be observed at least once by IUE with the large aperture, in low dispersion and with both, short-wavelength (SW) and long-wavelength (LW) cameras,
- to be observed spectrophotometrically in visual.

As a first step we folded the IUE archive with 5225 objects for which required observations exist with the *General Catalog of Ap and Am stars* by Renson et al. (1991). This step was necessary because not all CP stars observed with IUE are marked as such in the archive. 301 stars appear in both catalogs. They were checked against the following catalogs of visual scans: Adelman et al. (1989),Alekseeva et al. (1996, 1997), Breger (1976), Burnashev (1985), Glushnieva et al. (1998a,b) and Kharitonov et al. (1988). Observations exist for 137 stars from the previous sample in at least one of the visual catalogs. These stars were checked individually star by star and all non-CP2 stars were rejected. The final sample contains 27 stars. Apart from well known, classical mCP stars a few additional objects were included due to their peculiar character mentioned in literature. A closer analysis at a later stage of our investigation showed that not all of them belong to mCP stars but, nevertheless, we obtained their effective temperatures.

Table 1 lists all the investigated stars with their apparent peculiarities, magnitudes, accepted reddening, Strömgren reddening free indices and distances. Last six

Table 1. List of investigated stars.

HD	Other name	Pec.	V	$E(B-V)$	$[u-b]$	$[c_1]$	d(pc)	n(UV)	n(Ad)	n(Br)	n(Bu)	n(Gl)	n(Kh)
15089	ι Cas	Sr	4.53	0	1.350	0.866	43	12	9		1		1
19832	56 Ari	Si	5.77	0	0.786	0.560	114	90	23	2			1
23387	HII 717	CrSi	7.19	0	1.269	0.917	184	2					1
25823	41 Tau	SrSi	5.17	0	0.717	0.501	152	4	15	2	1	1	
26571	V1137 Tau	Si	6.15	0.27	0.720	0.512	316	11					1
27309	56 Tau	SiCr	5.35	0	0.892	0.559	97	4	4	1			
34452	IQ Aur	Si	5.37	0	0.648	0.374	137	10	24	1			1
37470	BD-06 1274	Si	8.23	0.15	0.892	0.668	265	3		1			
40312	θ Aur[a]	Si	2.62	0	1.239	0.974	53	23	20	1	2	1	1
43819	V1155 Ori	Si	6.27	0	1.019	0.762	193	1	5	1			
65339	53 Cam	SrEuCr	6.02	0	1.299	0.739	98	24	14				
92664	V364 Car	Si	5.50	0	0.583	0.403	143	10		1			
98664	σ Leo	Si	4.04	0	1.259	1.018	66	5			2	1	1
107966	13 Com	Am?	5.18	0	1.487	1.103	87	6			1	1	
108662	17 Com A	SrCrEu	5.24	0	1.289	0.891	83	7	4	1	1	1	
108945	21 Com	Sr	5.44	0	1.509	1.087	95	34	4	1			
112413	α^2 CVn	EuSiCr	2.90	0	0.976	0.641	34	34	29	2	1	1	1
118022	78 Vir	Cr EuSr	4.91	0	1.395	0.938	56	22	15	2	2	1	1
120198	84 UMa	EuCr	5.68	0	1.260	0.898	86	4	5				1
124224	CU Vir	Si	5.01	0	0.832	0.599	80	4	51	1	1	1	
125248	CS Vir	EuCr	5.86	0	1.364	0.926	90	7	15	0			
133029	BX Boo	SiCrSr	6.35	0	1.147	0.794	146	4	15	1			
144844	HR 6003	Si He-w	5.86	0.12	0.844	0.587	131	2		1			
152107	52 Her	SrCrEu	4.82	0	1.383	0.933	54	8		2	1	1	
171782	QV Ser	SiCrEu	7.85	0.17	0.999	0.742	286	2	4				
196502	73 Dra	SrCrEu	5.19	0	1.530	1.061	128	2	24				
215441	GL Lac	Si	8.81	0.26	0.568	0.315	714	16	15				

Ad - Adelman et al. (1989), Br - Breger (1976), Bu - Burnashev (1985), Gl - Glushnieva et al. (1998b), Kh - Kharitonov et al. (1988)

[a] Three more visual scans from Alekseeva et al. (1996, 1997) and Glushnieva et al. (1998a) were also included.

columns give the numbers of UV scans from IUE and visual scans from the respective catalogs used in the further analysis. Note that HD 192678, considered by Stępień & Dominiczak (1989), is missing here. This is because contradictory information on IUE observations of this star exists. In the *Final merged log of IUE observations* (*CDS Catalog VI/110*) HD 192678 appears with spectra SWP 7568 and LWR 6547 (which were used by Stępień & Dominiczak 1989). However, according to the *INES Catalog* (see below), these spectra are attached to HD 192679 which is only about 0.3 of a magnitude brighter than HD 192678 and has a spectral type of F5V. Apparent similarity of both stars might have caused the confusion. The Simbad database gives no mention of IUE observations for either star. We decided to exclude HD 192678 from our sample.

2.1 IUE Observations

The UV observations were extracted from *IUE Newly Extracted Spectra* (INES) *Catalog* in which the flux in absolute units (cgs) is given every 1.67 A for SW cameras and every 2.67 A for LW cameras. Observations were reduced with the use of the New Spectral Image Processing System (NEWSISP) method (Garhart et al. 1997). It is assumed, when reducing the observations, that those obtained with the large aperture contain a full stellar flux whereas only an unknown part of the flux is registered through the small aperture be-

cause of the vignetting effect. The precise calibration factor converting the small amplitude flux to the large aperture flux must be determined individually for each scan. Without large aperture observations such an individual factor cannot be found, so stars with only small amplitude spectra were excluded from our analysis.

As a first step, we checked all large aperture spectra for internal consistency. The following scans turned out to be discrepant: one SW scan of HD 19832 (out of 39 listed in archive), two SW scans of HD 34452 (out of 7), and 2 LW scans of HD 98664 (out of 3). In the last case the LW scans were additionally checked against SW and visual scans. All discrepant scans were rejected. Next, the average SED was formed from individual scans weighted with inverse square root of the observational error which is listed in the archive together with each measurement. Measurements flagged with negative "errors" are outliers and were not included into the average. Scaling factors for small aperture spectra were then determined from a comparison of a median value of each small aperture spectrum to a median value of the average large aperture spectrum. After multiplying all small aperture spectra by the corresponding scaling factors, they were averaged in the same way as those obtained with the large amplitude and compared with them. In no case any systematic difference between small and large amplitude spectra was detected, hence both sets were used to obtain the (weighted) grand average SED. Only one SW and one LW spectrum is available for HD 43819 and, un-

fortunately, the LW spectrum badly disagrees with the SW and visual scans. The discrepant spectrum was rejected but the star was retained. This is the only star in our analysis for which the full (i. e. UV plus visual) SED is not available. In the last step we calculated the values of the observed flux at the wavelengths for which model values are listed by Kurucz. The latter values are given every 10 A for wavelengths shorter than 2900 A and every 20 A for the longer ones. After dividing the observed spectral range into intervals with centers corresponding to the wavelengths in which model values of fluxes are given, the weighted average value for each interval was calculated. Fluxes in the overlapping wavelength interval were calculated from observations taken with both cameras, allowing for the respective errors. Thus obtained SEDs can directly be compared with theoretical models.

2.2 Visual observations

Adelman et al. (1989) list several scans for each observed star. The spectral passband varies between 25 and 30 A and the number of measurements per scan varies between 30 and 50. Fluxes are given in magnitudes and always centered at nearly the same wavelengths, although small differences among the scans are present. As a first step in forming the final SED we checked the scans of each star for internal consistency. For two stars: HD 171782 and HD 215441, additional scans corrected for interstellar absorption are also listed. We excluded them from further analysis because we applied the corresponding corrections to the whole SED of these stars (see below). Otherwise, the scans did not show discrepancies. Next, we reduced flux values of each star to a uniform set of wavelengths using linear interpolation. For example, if most of the observations were obtained for the wavelength 5556 but in some scans values for 5550 A are given, they were interpolated to the former wavelength. Then, mean SEDs were calculated assuming equal weights of all measurements. Scans of variable stars were obtained in different phases of the variation period so the mean SED can be treated as period averaged, particularly when a substantial number of scans is available. As a next step, the observations were converted into absolute units, using Vega calibration (Bohlin & Gilliland 2004)

$$F_\lambda = F_{\text{Vega},5556} \left(\frac{5556^2}{\lambda^2} \right) 10^{-0.4(V - V_{\text{Vega}} + m_\lambda - m_{5556})}, \quad (1)$$

where λ is the wavelength in A, F_λ is the stellar flux in absolute units (ergcm^{-2}s^{-1}A^{-1}), $F_{\text{Vega},5556} = 3.46 \times 10^{-9}$ ergcm^{-2}s^{-1}A^{-1}, V and $V_{\text{Vega}} = 0.026$ are the magnitudes of the star and Vega in V-band of the UBV system, and m_λ and m_{5556} are the magnitudes of the star at the wavelength λ and at 5556 A.

If, instead of averaging magnitudes, we had transformed them into fluxes, the resulting differences in the mean values turned out to be negligible (less than 0.5 %), compared to the procedure described above.

Breger (1976) lists observations obtained by many different observers and with different instrumentation. Bandwidths used by them extend from 10 to 100 A. For eleven stars the catalog contains only one scan and for 5 of them two scans per star, extending over different spectral regions,

e.g. 3000 - 5500 A and 5000 - 8000 A. The analyzed scans were first compared to those from the Adelman et al. catalog (if the latter were available). Only in case of one scan of HD 112413 a substantial discrepancy occurred. This scan was also discordant with the UV observations so we rejected it. All the accepted scans were then reduced to absolute units in the same way as those from Adelman et al. catalog and merged into one SED by averaging measurements from overlapping spectral intervals if two scans were available.

In the catalogs of Alekseeva et al. (1997), Burnashev (1985), Glushnieva et al. (1998a,b) and Kharitonov et al. (1988) (henceforth ABGK catalogs) from 1 to 7 scans per star are given. Alekseeva et al. (1997) used the bandwidth of 100 A. We could not find any information on bandwidths used by the other authors. Nearly all the observations extend from 3200 to about 8000 A but Alekseeva et al. (1997) and Glushnieva et al. (1998a) obtained observations up to 10800 A. For consistency with other observations we ignored observations beyond 8500 A. The fluxes listed in the ABGK catalogs are given in absolute units per different length units. To reduce them to the common scale we applied corresponding scaling factors. Next, fluxes of each star were interpolated to a uniform wavelength set and averaged, assuming equal weights.

In all the considered catalogs the observations obtained within the Balmer lines or very close to them are present. Because we are interested in continuum distribution only, the observations affected by Balmer lines were rejected. The remaining continuum observations were interpolated to the wavelengths listed in model computations.

Because the scans from Adelman et al. (1989) and Breger (1976) are given on the same scale, a direct comparison of them for each star can be made. No systematic difference was found between both sets of scans for stars listed in the catalogs. A good agreement means that the temperatures obtained for stars not observed by Adelman et al. (1989) but present in the Breger catalog do not need any systematic corrections. Scans from the ABGK catalogs could not be directly compared with those from Adelman et al. or Breger catalogs, so they were analyzed separately to keep track of any possible systematic differences. The results showed that they also agree well with the Adelman et al. and Breger catalogs (see below).

2.3 IUE + visual SED

When a UV spectrum is plotted together with a visual scan, they usually do not merge smoothly. Instead, a gap is often visible between them in the wavelength region around 3200 A covered by both sets of observations. Visual observations were retained here because formal errors of the UV observations in the overlapping region are substantially larger than those of visual observations. In majority of cases the UV observations lie slightly lower than visual but there are also cases when they agree well and even some cases when they lie higher. Small shifts between UV and visual observations result probably from calibration errors. No attempt was made to remove them.

The observed SED should be corrected for interstellar absorption before fitting the theoretical SED. Unfortunately, standard methods of determination the individual values of the interstellar reddening cannot be applied to

Table 2. Effective temperatures of stars common in Ad+Br and ABGK catalogs.

HD	T_e(Ad+Br)	T_e(ABGK)	ΔT_e
15089	8250	8500	-250
19832	12750	13000	-250
25823	13250	13500	-250
34452	14750	15000	-250
40312	10500	10250	250
108662	10250	9750	500
112413	11750	12000	-250
118022	9000	9250	-250
120198	10500	10500	0
124224	13000	13250	-250
152107	8750	8500	250

mCP stars due to their peculiar photometric indices (Wolff 1967; Stępień & Muthsam 1980). Other, indirect methods, e. g. based on maps of the distribution of the interstellar matter, can also result in gross errors because interstellar dust has a very patchy structure. Recent investigation of interstellar absorption for many W UMa-type stars by Rucinski & Duerbeck (1997) showed that the reddening of nearby stars had been significantly overestimated by earlier authors. In fact, interstellar reddening is close to zero for stars closer than 100 pc and rarely exceeds 0.03 for distances up to 200 pc (see also Fruscione et al. 1994). Based on these results we assumed zero reddening for all stars closer than 100 pc. Each star lying further than 100 pc was checked individually. If literature data or maps of interstellar matter suggested $E(B-V) \leqslant 0.03$ we assumed zero reddening. We believe that the overestimate of the reddening is as dangerous for the determination of true SED as its underestimate, so in cases when no lower limit for the reddening is given, it is safer to assume zero. Several stars are, however, significantly reddened and values of $E(B-V)$ up to 0.27 mag can be found in literature. With one exception we accepted the literature values as they are, although some of them are very uncertain. For one star, HD 215441, the fit of the model atmosphere was so poor with the published $E(B-V) = 0.20$ that we decided to do a numerical experiment for this star by keeping the reddening as an additional free parameter to be determined from the best fit (see 3.1). The observed SEDs of reddened stars were corrected for interstellar extinction using the curve given by Cardelli et al. (1989), see also Fitzpatrick & Massa (2007). The accepted values of $E(B-V)$ are listed in Table 1 with references given in the comments to individual stars. As a final step before fitting theoretical SED, the observed fluxes were converted to units used by Kurucz.

3 RESULTS

3.1 Effective temperatures

The root-mean-square (RMS) method was used to fit a theoretical SED to observations of each star. Equal weights were given to the UV and visual part of SED. Because the numbers of matching points are different in both spectral regions, weights of individual points were equal to n_{UV}^{-1} and n_{vis}^{-1}, where n_{UV} and n_{vis} are, respectively, the numbers of matching points in the UV and visual scan of the considered star.

If $\{f_i\}$ denote the observed values of the flux and $\{F_i\}$ the theoretical flux values from the model, we look for a (linear) factor a such that $\mathbf{f} = a\mathbf{F}$ gives the best RMS fit. The root mean square error (RMSE) σ is a measure of the quality of fit

$$\sigma = \sqrt{\frac{\sum (f_i - aF_i)^2}{n-1}}, \qquad (2)$$

where n is a number of fitting points. A theoretical SED depends on three basic parameters: effective temperature, metallicity and surface gravity. It is known, however, that the effective temperature is the primary parameter influencing SED. Variations of SED due to variations of gravity or metallicity are of the second order (compared to temperature variations). Moreover, they are correlated in a sense that a change of the model SED due to decreased metallicity can be compensated by the increased gravity (at constant effective temperature), and *vice versa*. If reddening is treated as an additional free parameter, our calculations show that there exists a trade-off between it and the stellar parameters. As a result, the absolute minimum of RMSE may be spurious and a secondary minimum should be considered as more reliable. That happened to HD 215441 (see below).

Even with reddening fixed, a simultaneous determination of temperature, metallicity and gravity is not possible, at least in case of mCP stars. Surface gravity of these stars is usually determined from other observations, e. g. profiles of Balmer lines or β-index (Adelman & Rayle 2000). Unfortunately, the Balmer line profiles in mCP stars are subject to modifications due to the Lorentz force influencing the effective gravity in high atmospheric layers (Stępień 1978). As a result, their intensity often varies with rotation phase (Musielok & Madej 1988). Gravity determined from such lines is more uncertain than in case of non-magnetic stars. All available observational data indicate, nevertheless, that most, if not all, mCP stars are main sequence (MS) objects, which means that their values of $\log g$ concentrate around 4.0 with a scatter of about $\pm$ 0.3-0.4 (see e. g. Adelman & Rayle 2000). We assumed therefore $\log g = 4.0$ for all investigated stars except two giants, HD 26571 and HD 43819, for which $\log g = 3.0$ was adopted based on their spectral class. It should be stressed, nevertheless, that the models with $\log g = 4.0$ and metallicity increased by 0.5dex fit the observations of both giants as well as the accepted models. Fortunately, the obtained effective temperatures are insensitive to such variations of model parameters.

With gravity fixed, the effective temperature and metallicity were varied when fitting models to observations, i. e. $\mathbf{F} = \mathbf{F}(T_e, \mathrm{m/H})$. The best fitting values of the parameters were determined from the σ minimum. A typical minimum was rather broad – the change of metallicity by 0.5 dex and/or effective temperature by 250 K resulted in a change of RMSE by 5-10 %, which shows that the actual accuracy of the optimum values of T_e and [m/H] is of that order. Eleven stars are common in Ad+Br and ABGK catalogs (see Table 1). For them separate fits were obtained to visual scans taken from the respective catalogs (without IUE scans). Table 2 lists the results. The average difference between temperatures based on both groups of catalogs is about -70 K which is negligible. We conclude that no sys-
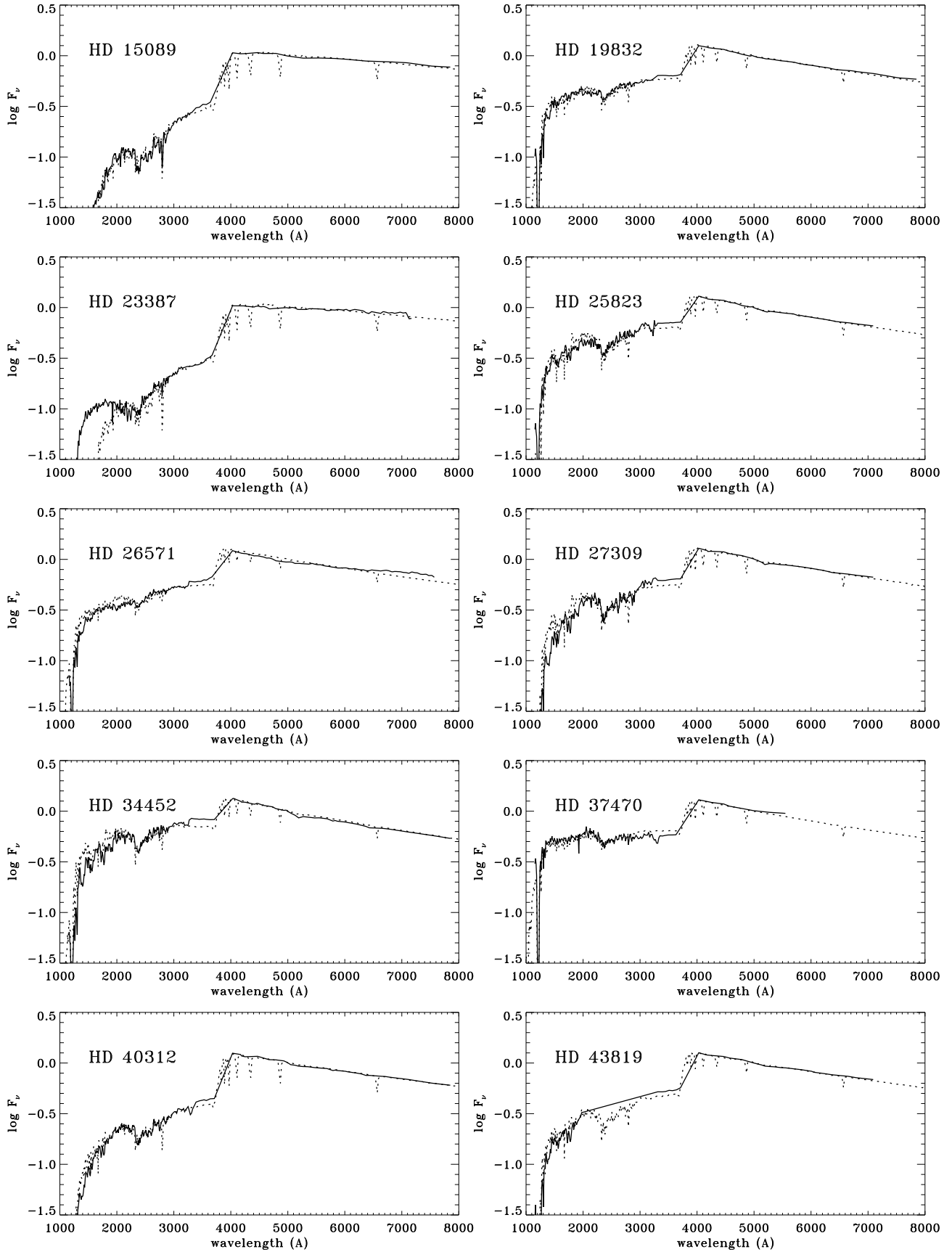
Figure 1. The observed SED (solid lines) with the best fitting models (broken lines).
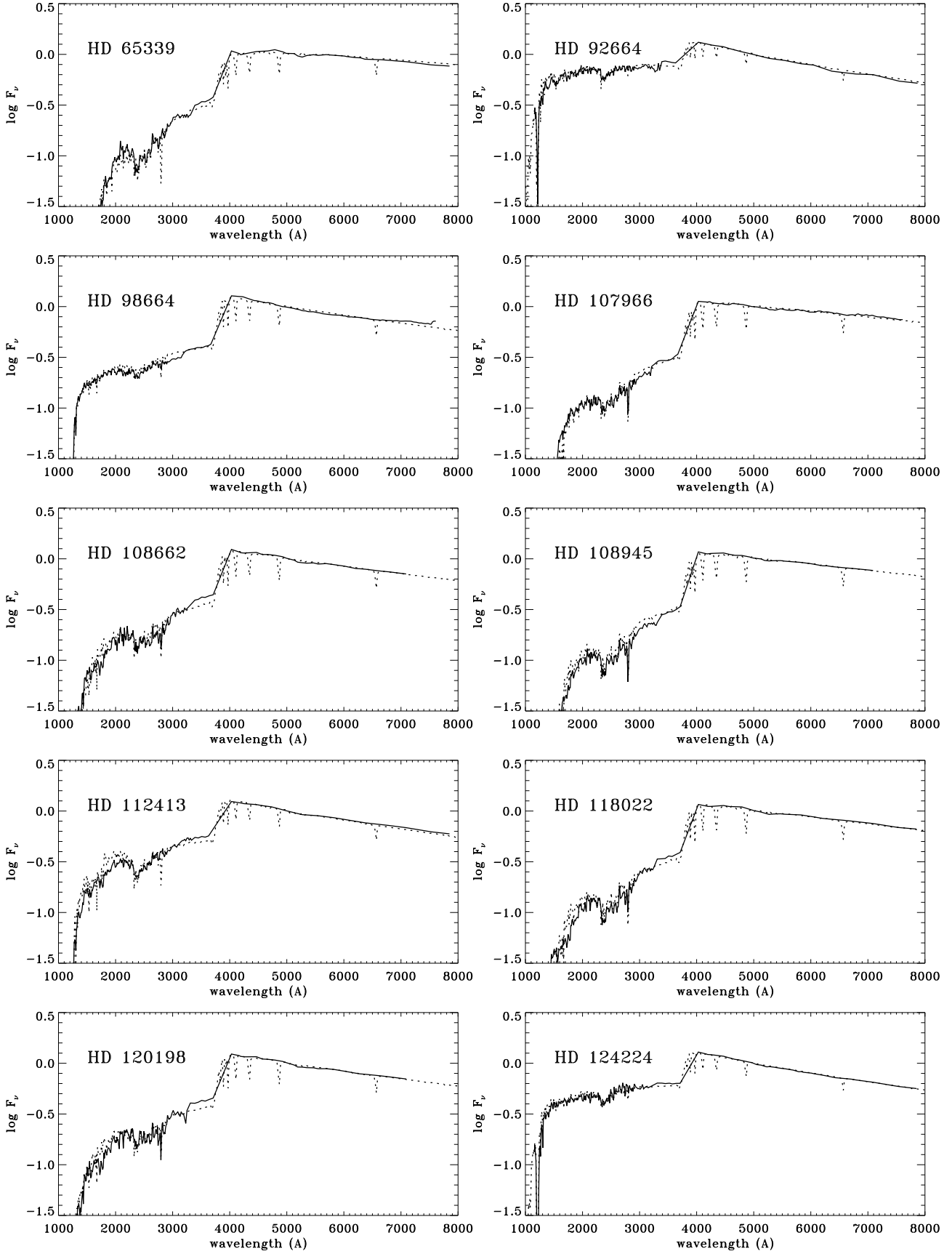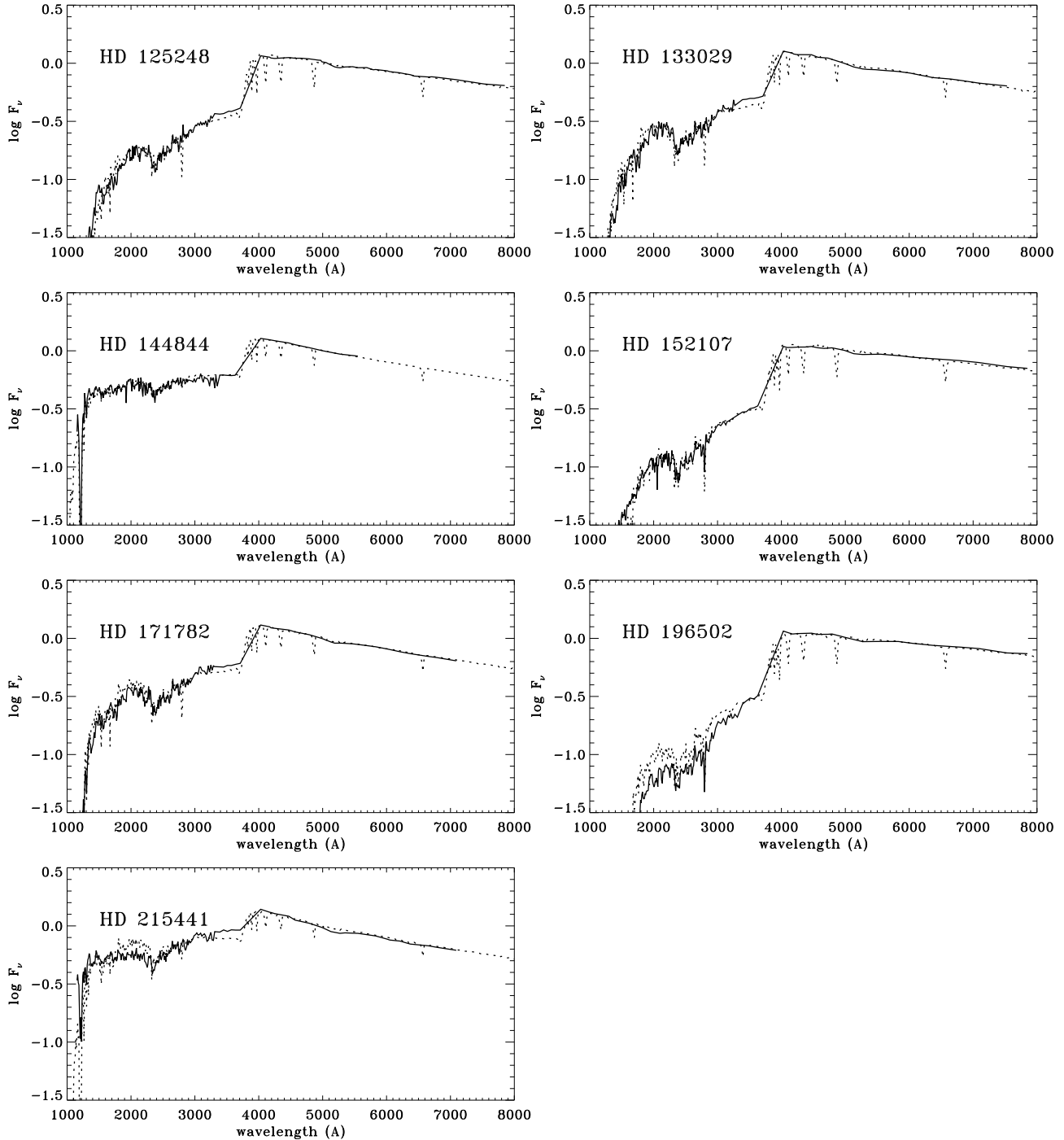
Figure 1. – continued.

Figure 1. – concluded.

tematic difference exists between spectrophotometric data from Ad+Br and ABGK catalogs. The latter catalogs were used together with IUE data to determine the effective temperatures of HD 23387, 26571, 98664 and 107966.

HD 215441 was treated in a special way. The best fit to its full SED corrected for the interstellar reddening $E(B-V) = 0.20$ (Stępień 1968) resulted in metallicity of 1.0 and the effective temperature of 13 000 K. However, the quality of fit was extremely poor. The theoretical model showed a substantially higher Balmer jump than observations and a dif-

ferent slope of the Paschen continuum. Also the UV part of SED was poorly reproduced. In addition, a fit of theoretical models separately to the visual part of SED and then to the UV part of SED gave the temperatures equal to 14 750 K and 14 000 K, respectively, i.e. significantly higher than that resulting from the best fit to the full SED (see below). We decided therefore to treat the reddening as an additional free parameter and to determine it from the best fit together with metallicity and effective temperature. The procedure turned out to be only partly satisfactory. The lowest value

of RMSE (normalized to the total flux) was obtained for [m/H] = 0.5, T_e = 16 000 K and $E(B - V)$ = 0.37. We think that such values are unreliable and they result most likely from a correlation between the influence of [m/H] and $E(B - V)$ on SED (similarly as it is in case of [m/H] and log g). Because of that, both parameters cannot be simultaneously determined together with the effective temperature from the SED alone. To get rid of degeneracy we *adopted* [m/H] = 1.0 and looked then for minimum of RMSE by varying effective temperature and reddening only. The best fit was obtained for $E(B - V)$ = 0.26 and T_e = 14 000 K. We consider the fit as physically feasible and we accepted it as our final result although some discrepancies still remain (see Fig. 1).

Table 3 lists the final temperatures and metallicities resulting from fits to full SEDs and Fig. 1 shows the observed SEDs with the best fitting models. With known T_e, angular diameters of the investigated stars were calculated from the equation

$$\theta = \sqrt{\frac{4f_t}{\sigma T_e^4}}\,, \tag{3}$$

where σ is the Stefan-Bolzmann constant and f_t is the integrated observed flux. From angular diameters and distances stellar radii in solar units can be obtained (Table 3).

Earlier determinations of the effective temperatures of mCP stars, based on the observed SED were collected and discussed by Stępień (1994). 15 stars from that paper are in common with the present investigation. Fig. 2 compares effective temperatures of these stars. Diagonal is shown as a solid line. As can be seen from the figure, older determinations agree satisfactorily with the present ones but a small systematic difference between them appears in a sense that the older temperatures are on average hotter by 190 K. The difference is within the uncertainty of the temperature determination and probably reflects the slightly better description of the metal opacity in UV by the recent models, compared to earlier ones.

3.2 Uncertainties

As it was mentioned earlier, the uncertainty of the best fit, estimated from the shape of the minimum of RMSE is of the order of 200-300 K. It can be seen from Fig. 1, however, that while in some cases the observed SEDs agree very well with the best fitting models, there are also cases where the fit is rather poor (e. g. HD 34452 or 215441). Uncertainty of each individual determination of the effective temperature should reflect this quality of fit. To measure it quantitatively, models were fitted separately to the UV scan of each star and then to the visual scan. Gravity and metallicity were the same as in the global best fitting models to the full SEDs and were kept fixed. Table 3 shows the results. In majority of cases temperature found from the visual scan is higher than from the UV scan but in several stars it is lower. The difference $T(\text{vis}) - T(\text{UV}) = \Delta T$ is plotted versus T_e and [m/H] in Fig. 3. Note that any possible uncertainties of UV calibration relative to the visual observations (suggested by apparent gaps between both scans visible in some stars) have no influence on thus found temperatures - only the shape of SED matters. In a case of the perfect fit between the theoretical model and observations, separate fits to UV and visual
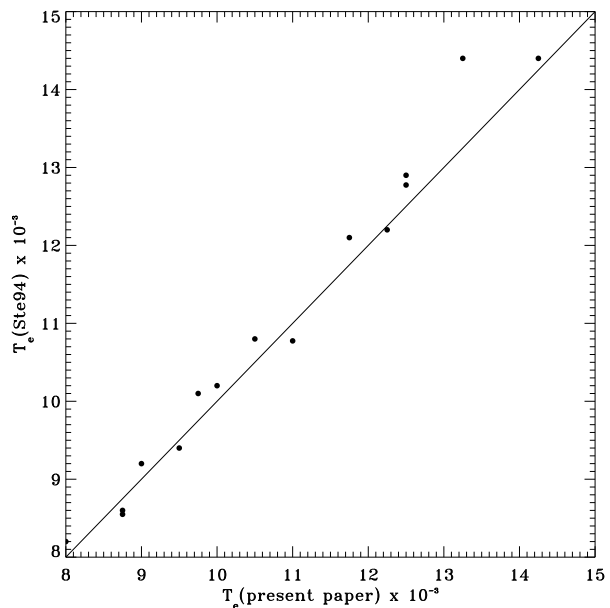

Figure 2. A comparison of effective temperatures from the present paper with temperatures listed by Stępień (1994).

scan should give identical temperatures or, at most, differing by a value of the estimated error from the best fit to the full SED which, in nearly all cases, lies between $T(\text{vis})$ and $T(\text{UV})$. That means that the difference $|\Delta T| \leqslant 500$ K (i. e. twice the error) indicates a satisfactory quality of fit. This occurs in 11 stars. In addition, there are 5 "border cases" with $|\Delta T| = 750$ K. In all other stars it exceeds that value and the most extreme differences reach -2250 K and 3000 K. Such large differences indicate that the best fitting models do not yet give satisfactory results. A closer inspection of SEDs of stars with apparently close effective temperatures, e. g. HD 34452 and HD 37470 (Fig. 1), reveals, indeed, profound differences in shapes of UV spectrum, which result from a different UV line blanketing between both stars. Obviously, scaled solar abundances are a very poor alternative of the true chemical compositions. The largest positive values of ΔT are present in stars with the highest available metallicity as can be seen from Table 3 and Fig. 3. This indicates that the solar metallicity enhanced by a factor of 10 is still insufficient to correctly reproduce the observed SED. Perhaps models with [m/H] = 1.5 or even 2.0 would do it better. Note that Leckrone et al. (1974) adopted line opacity enhanced by a factor of 100 to qualitatively reproduce differences between normal and Ap star flux distributions. Substantial discrepancies between $T(\text{UV})$ and $T(\text{vis})$ do not necessarily mean that the present effective temperatures are in gross error. Future models with individually adjusted chemical compositions will simply narrow an existing gap between these two temperatures, although they may close the gap at a somewhat different value of effective temperature than the present one. Large negative differences appear for two stars: HD 23387 and HD 37470. The former star shows unusually flat Paschen continuum which results in low $T(\text{vis})$. Such flat or, sometimes, rounded continua with a depression at the short wavelength end appear in a few Ap stars during all, or some of the phases of the rotation
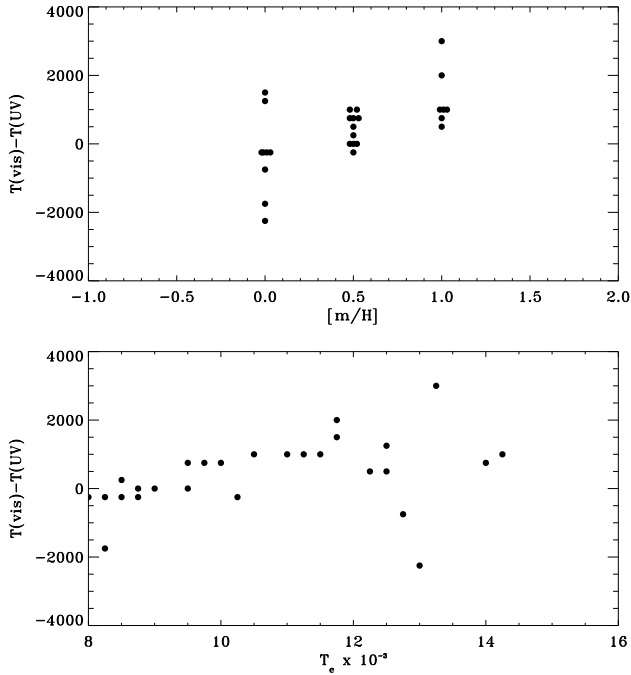
Figure 3. The dependence of $\Delta T = T(\text{vis})$ - $T(\text{UV})$ on metallicity (top) and effective temperature (bottom).

period (Kodaira 1973; Pyper & Adelman 1983) due to a very strong blanketing effect concentrated in this spectral region. That makes the Paschen continuum of such stars look unusually flat. This does not seem, however, to be the case for HD 23387 which is, at most, mildly peculiar, or may even be normal (Landstreet et al. 2007). At present we cannot offer a convincing explanation for the existing discrepancy. Obviously, new, more accurate observations of this star are needed. The other star, HD 37470, was observed in visual up to 5500 A only. In addition, the red end of the Paschen continuum looks unusual (see Fig. 1), so it is possible that the uncertain visual scan is responsible for the discrepancy.

In one star, HD 25823, the best fitting temperature is *lower* than either $T(\text{UV})$ or $T(\text{vis})$. This unexpected result is most likely due to a particularly large mismatch of both parts of SED. If the UV SED is too faint compared to visual SED, the best fitting model will also give a too low temperature compared to the temperatures resulting from separate fits to UV and visual parts of SED. Conversely, too bright UV SED compared to the visual SED results in a too high best fitting value of the temperature. For HD 25823 the best fitting temperature is lower by 250 K than $T(\text{UV})$ and by 750 K than $T(\text{vis})$, so that all three temperatures are within 2-3 σ from each other. In several other stars the best fitting temperature is very close to, or identical with one of the temperatures found from the UV or visual scan. This may also be the result of a small mismatch of both parts of SED.

An additional source of uncertainty of effective temperatures of the investigated stars is connected with poorly known reddening corrections. The accepted $E(B - V)$ values may in some cases be in error up to a few hundredths of magnitude. The best fitting temperature increases by about 1 % per 0.01 mag increase of $E(B - V)$ as our numerical experiment showed. Assuming that $E(B - V)$ may be in error

up to 0.03 mag we obtain the value of about 250 - 400 K for the maximum error of effective temperature resulting from poorly known reddening.

Variability, ubiquitously observed in mCP stars, may result in apparent temperature variations with rotational phase (Muthsam & Stępień 1980; Stępień & Muthsam 1987). Our final temperatures can be affected by such variations, particularly for stars with few scans unfavorably distributed in phase.

As it is seen, all the discussed error sources have a highly various, and difficult to assess, importance for individual stars. Therefore, instead of trying to determine the uncertainty for each star separately, we estimate an *average* uncertainty at about 500 K.

3.3   Comments on individual stars.

Approximate values of variability periods P_{rot} and average effective magnetic fields are taken from Bychkov et al. (2003, 2005), unless otherwise indicated.

HD 15089, $P_{\text{rot}} = 1.74$ d and $\overline{B_e} = 200$ G.

HD 19832, $P_{\text{rot}} = 0.73$ d and $\overline{B_e} = 300$ G.

HD 23387, Pleiades member, unknown rotation period, $\overline{B_e} = 1.8$ kG. Landstreet et al. (2007) considers the star as normal with no magnetic field.

HD 25823, $P_{\text{rot}} = 4.66$ d and $\overline{B_e} = 700$ G.

HD 26571, B9IIIp, reddening from Isobe et al. (1986),$P_{\text{rot}} = 15.7$ d, mag. field ?

HD 27309, $P_{\text{rot}} = 1.11$ d and $\overline{B_e} = 1.8$ kG.

HD 34452, $P_{\text{rot}} = 2.47$ d and $\overline{B_e} = 700$ G.

HD 37470, reddening from Schild & Chaffee (1971), unknown rotation period, $\overline{B_e} = 160$: G.

HD 40312, $P_{\text{rot}} = 3.62$ d and $\overline{B_e} = \sim 500$ G, radius $R = 3.6 R_{\odot}$ (Borra & Landstreet 1980).

HD 43819, B9IIIp, $P_{\text{rot}} = 15.03$ d (Adelman & Young 2005), $\overline{B_e} = 300$ G.

HD 65339, $P_{\text{rot}} = 8.03$ d and $\overline{B_e} = 3$ kG, binary with $P_{\text{bin}} = 2400$ d. Nearly identical components with masses $M_{1,2} = 1.5 M_{\odot}$ (Carrier et al. 2002).

HD 92664, $P_{\text{rot}} = 1.67$ d and $\overline{B_e} = 800$ G.

HD 98664, unknown rotation period, mag.field?, normal star?

HD 107966, member of Coma cluster, SB?, $P_{\text{rot}} > 1$ d (Jackisch 1972), mag. field?, Am?

HD 108662, member of Coma cluster, blue straggler?, $P_{\text{rot}} = 5.08$ d and $\overline{B_e} = 600$ G, mass $M = 2.4 M_{\odot}$ (Casewell et al. 2006).

HD 108945, member of Coma cluster, $P_{\text{rot}} = 1.92$ d and $\overline{B_e} = 500$ G, mass $M = 2.4 M_{\odot}$ (Casewell et al. 2006).

HD 112413, $P_{\text{rot}} = 5.47$ d and $\overline{B_e} = 1.3$ kG.

HD 118022, $P_{\text{rot}} = 3.72$ d and $\overline{B_e} = 800$ G.

HD 120198, $P_{\text{rot}} = 1.39$ d and $\overline{B_e} = 700$ G.

HD 124224, $P_{\text{rot}} = 0.52$ d and $\overline{B_e} = 600$ G.

HD 125248, $P_{\text{rot}} = 9.30$ d and $\overline{B_e} = 1.5$ G, $R = 1.97 R_{\odot}$ (Bagnulo et al. 2002).

HD 133029, $P_{\text{rot}} = 2.11$ d and $\overline{B_e} = 2.5$ G.

HD 144844, reddening from Gordon et al. (1994), unknown rotation period, $\overline{B_e} = 300$ G.

HD 152107, UMa moving group, SB with a faint secondary (King et al. 2003), $P_{\text{rot}} = 3.87$ d and $\overline{B_e} = 500$ G.

Table 3. Final results.

HD	[m/H]	T_e(final)	Θ	BC	T(vis)	T(UV)	ΔT	$f_t \times 10^7$	θ(mas)	$R/R_\odot$
15089	0.0	8250	0.611	-0.01	8250	8500	-250	3.86	0.50	2.3
19832	0.5	12250	0.411	-0.74	12750	12250	500	2.43	0.18	2.1
23387	0.0	8250	0.611	-0.05	8000	9750	-1750	0.347	0.15	2.1
25823	1.0	12500	0.403	-0.67	13250	12750	500	3.94	0.22	3.6
26571	0.0	11750	0.429	-0.76	12250	10750	1500	3.66	0.24	8.1
27309	1.0	11750	0.429	-0.58	12500	10500	2000	3.07	0.22	2.3
34452	1.0	13250	0.380	-0.80	14750	11750	3000	3.71	0.19	2.9
37470	0.0	13000	0.388	-0.96	12250	14500	-2250	0.466	0.07	1.9
40312	0.5	10000	0.504	-0.26	10500	9750	750	28.2	0.92	5.2
43819	0.5	11000	0.458	-0.38	11250	10250	1000	1.10	0.15	3.2
65339	0.0	8000	0.630	-0.02	8000	8250	-250	0.995	0.27	2.8
92664	0.5	14250	0.354	-1.01	15250	14250	1000	3.97	0.17	2.7
98664	0.0	10250	0.492	-0.28	10250	10500	-250	7.78	0.46	3.3
107966	0.0	8500	0.593	-0.07	8500	8750	-250	2.25	0.36	3.3
108662	0.5	9500	0.531	-0.15	10250	9500	750	2.28	0.29	2.6
108945	0.5	8750	0.576	0.01	8750	8750	0	1.64	0.29	3.0
112413	1.0	11250	0.448	-0.42	11750	10750	1000	25.4	0.69	2.5
118022	0.5	9000	0.560	-0.05	9000	9000	0	2.83	0.36	2.2
120198	0.5	9750	0.517	-0.20	10500	9750	750	1.59	0.23	2.2
124224	0.0	12500	0.403	-0.79	13000	11750	1250	5.08	0.25	2.2
125248	0.5	9500	0.531	-0.17	9500	9500	0	1.31	0.22	2.1
133029	1.0	10500	0.480	-0.40	11250	10250	1000	1.04	0.16	2.4
144844	0.0	12750	0.395	-0.77	12750	13500	-750	3.18	0.19	2.7
152107	0.5	8750	0.576	-0.01	8750	9000	-250	2.97	0.39	2.3
171782	1.0	11500	0.438	-0.53	12000	11000	1000	0.472	0.09	2.7
196502	0.5	8500	0.593	-0.02	8500	8250	250	2.13	0.35	4.8
215441	1.0	14000	0.360	-0.80	14750	14000	750	0.32	0.05	4.2

HD 171782, reddening from Adelman (1980), $P_{\rm rot} = 4.47$ d (Paunzen & Maitzen 1998), mag. field?

HD 196502, $P_{\rm rot} = 20.3$ d and $\overline{B_e} = 500$ G.

HD 215441, reddening from the present paper, mass $M = 3 - 4M_\odot$ (Landstreet et al. 1989), $P_{\rm rot} = 9.49$ d, $\overline{B_e} = 17$ kG.

3.4 Revised photometric calibrations

All the analyzed stars have been measured in the Strömgren photometric system so reddening free indices $[u-b]$ and $[c_1]$ can be calculated for them (see Table 1). They are defined as

$$[u - b] = (u - b) - 1.53(b - y), \qquad (4)$$

$$[c_1] = c_1 - 0.20(b - y). \qquad (5)$$

Figure 4 presents the dependence of the parameter $\Theta = 5040/T_e$ on $[u - b]$ (top) and on $[c_1]$ (bottom). The data clearly show that quadratic fits are required to describe satisfactorily both dependencies. The calculations confirm indeed that the quadratic terms are significant. Four stars, marked with squares, were excluded from the best fits. Three high lying symbols correspond to three coolest stars from the sample, with temperatures below 8500 K. Both Strömgren indices are sensitive to the height of the Balmer jump, hence they are good measures of temperature only for stars hotter than about 8500 K, i.e. as long as the height of the Balmer jump increases monotonically with decreasing temperature. Beyond this temperature the jump *decreases* with a decreasing temperature, which is reflected by an apparent shifting of such stars on the index-temperature diagrams towards

lower values of the indices as visible in the Fig. 4. Fourth star, HD 98664, is apparently a normal star (see the comments above).

The best fit to the data in the $[u - b]$ - Θ diagram is given by

$$\Theta = 0.3167 + 0.0284[u - b] + 0.1017[u - b]^2, \qquad (6)$$
$$0.55 < [u - b] < 1.55.$$

Earlier calibrations were linear in $[u-b]$ so, for the sake of comparison, we also fitted a straight line to the data. The result is

$$\Theta = (0.2121 \pm 0.0131) + (0.2442 \pm 0.0120)[u - b], \qquad (7)$$

We give four significant digits for the straight comparison of our result with Napiwotzki et al. (1993), although it is clearly seen that the last digits are meaningless. Their relation

$$\Theta = 0.2162 + 0.2301[u - b], \qquad (8)$$

and the relation derived by Stępień (1994)

$$\Theta = 0.200 + 0.246[u - b], \qquad (9)$$

differ insignificantly from the presently derived linear fit. It means that both older calibrations are not grossly erroneous. The quadratic fit refines, however, the existing calibrations.

Similarly, the best quadratic fit to the data in the $[c_1]$ - Θ diagram is given by

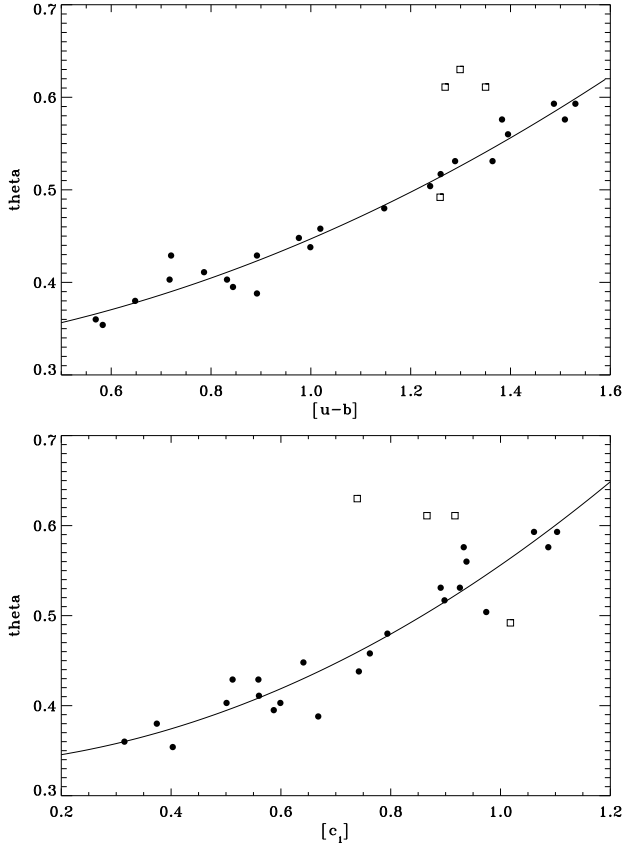$$\Theta = 0.3328 + 0.0237[c_1] + 0.1996[c_1]^2, \qquad (10)$$

Figure 4. A new calibration of Strömgren reddening free photometric indices in terms of effective temperature of the MCP stars. Best fitting lines are described in the text.
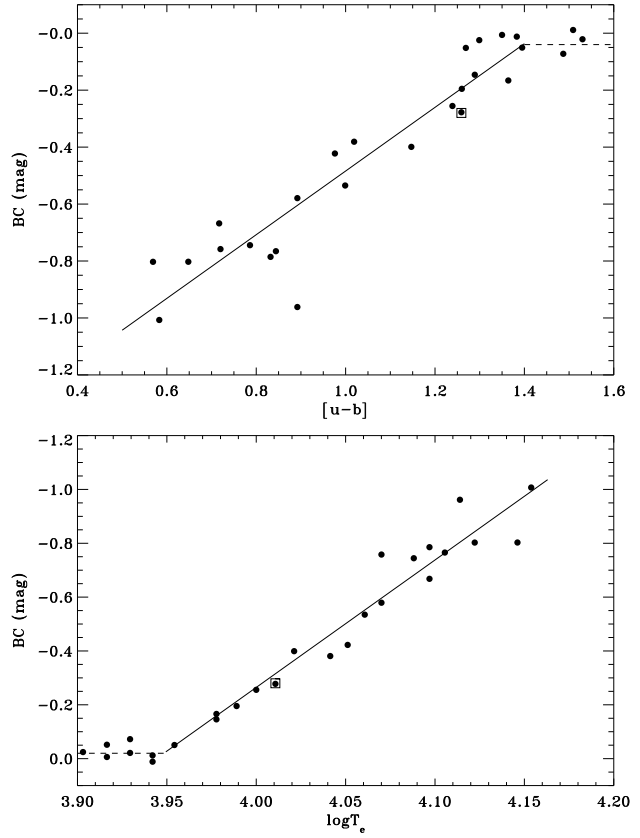

Figure 5. A new calibration of bolometric correction for MCP stars in terms of reddening free index $[u - b]$ (top) and effective temperature (bottom). Best fitting lines are described in the text.

$$0.3 < c_1 < 1.1 \,.$$

The linear fit

$$\Theta = (0.2382 \pm 0.0179) + (0.3136 \pm 0.0233)[c_1] \,, \qquad (11)$$

can be compared with Napiwotzki et al. (1993)

$$\Theta = 0.2489 + 0.2698[c_1] \,. \qquad (12)$$

From f_t one can find the apparent bolometric magnitude $m_{\rm bol}$ of a star using the relation given by Code et al. (1976)

$$m_{\rm bol} = -2.5 \log f_t - 11.51 \,. \qquad (13)$$

The difference between $m_{\rm bol}$ and the apparent stellar visual magnitude (corrected for reddening) gives the bolometric correction BC. The bolometric corrections for the investigated stars are listed in Table 3 and plotted in Fig. 5 as a function of $[u - b]$ (top) and effective temperature (bottom). The best fitting relations are also plotted. Because HD 98664 lies very close to the best fitting lines in both diagrams, it has a negligible influence on the best fits. It is marked with a square overplotted on a solid circle and was included in the fit. Solid lines give best linear fits to the data excluding the coolest stars which all have $BC \approx 0$. A quadratic term in both cases turned out to be insignificant. The solid lines are described by

$$BC \;\; = \;\; (-1.602 \pm 0.092) + (1.118 \pm 0.086)[u - b] \qquad (14)$$

$$0.5 < [u - b] < 1.4 \,,$$

and by

$$BC \;\; = \;\; (18.668 \pm 0.975) - (4.733 \pm 0.241) \log T_e \,, \qquad (15)$$
$$3.94 < \log T_e < 4.16 \,.$$

4   CONCLUSIONS

Effective temperatures were determined for 27 stars. All but HD 98664, possess at least two properties characteristic of mCP stars, i.e. chemical peculiarities, light variations and/or measurable surface magnetic field. The temperatures were found from a fit of a metal enhanced model atmosphere to the full SED, including UV spectrophotometry from IUE and visual scan from ground based observations. In case of distant stars the observed SEDs were corrected for reddening before searching the best fitting model. Our experience with fitting models to observations showed that reliable results can be obtained only when at most two free parameters describing a model are used in the best fit, e.g. metallicity and temperature. Introducing the third unknown parameter, e.g. reddening or gravity, to be determined from the best fit simultaneously with the other two produces either indeterminacy or gives a spurious result. We assumed therefore $\log g = 4$ for all main sequence stars and $\log g = 3$ for two known

giants. We also adopted individual values of $E(B-V)$ from literature or assumed zero reddening for close stars. In one case of HD 215441 we attempted to determine the value of $E(B-V)$ from the best fit. However, to obtain meaningful results we were forced to keep metallicity fixed when fitting models to the observations. In addition to fitting a model to the full SED we also fitted a model separately to the UV and the visual part of SED of each star. A difference between thus found temperatures is a measure of quality of fit to the full SED. In about a half of stars the difference is small enough to consider the fit acceptable but in the remaining stars the difference was $\geqslant 1000$ K which indicates a necessity to improve the atmospheric models of mCP stars. The presently available models reproduce the observations only approximately. Taking into account all uncertainties, we estimate an error of determination of effective temperature at 500 K.

Together with Strömgren photometry, new determinations of the effective temperatures were used to produce improved color-temperature calibrations for mCP stars. New data suggest quadratic calibration formulas in color indices. From total integrated fluxes bolometric corrections were computed and improved color-BC and temperature-BC calibrations were also determined.

REFERENCES

Adelman S.J., 1980, A&AS, 42, 375
Adelman S.J., Young K.J., 2005, A&A, 429, 317
Adelman S.J., Rayle K.E., 2000, A&A, 355, 308
Adelman S.J., Pyper D.M., Shore S.N., White R.E., Warren W.H., 1989, A&AS 81, 221
Alekseeva G.A. et al., 1996, Baltic Astron., 5, 603
Alekseeva G.A. et al., 1997, Baltic Astron., 6, 481
Bagnulo S., Landi Degl'Innocenti M., Landorfi M., Mathys G., 2002, A&A, 394, 1023
Blackwell D.E., Shallis M.J., 1977, MNRAS, 180, 177
Bohlin R.C., Gilliland R.L., 2004, AJ, 127, 3508
Borra E.F., Landstreet J.D., 1980, ApJS, 42, 421
Breger, M., 1976, ApJS, 32, 7
Burnashev, V.I., 1985, Abastumanskaya Astrofiz. Obs. Bull., 59, 83
Bychkov V.D., Bychkova L.V., Madej J., 2003, A&A, 407, 631
Bychkov V.D., Bychkova L.V., Madej J., 2005, A&A, 430, 1143
Cardelli J.A., Clayton G.C., Mathis J.S., 1989, ApJ, 345, 245
Carrier F., North P., Udry S., Babel J., 2002, A&A, 394, 151
Casewell S.L., Jameson R.F., Dobbie P.D., 2006, MNRAS, 365, 447
Code A.D., Bless R.C., Davis J., Brown R.H., 1976, ApJ, 203,417
Fitzpatrick E.L., Massa D., 2007, ApJ, 663, 320
Fruscione A., Hawking I., Jelinsky P., Wiercigroch A., 1994, ApJS, 94, 127
Garhart M.P., Smith M.A., Turnrose B.E., Levay K.L., Thompson R.W., 1997, NASA IUE Newsletter, No. 57, 1
Glushnieva I.N. et al., 1998a, Moscow Spectrophotometric Catalog of Stars, Moscow
Glushnieva I.N. et al., 1998b, Spectrophotometric Catalog of Stars of the Sternberg Institute, Moscow
Gordon K.G., Witt A.N., Carruthers G.R., Christensen S.A., Dohne B.C., 1994, ApJ, 432, 641
Hauck B., Künzli M., 1996, Baltic Astron., 5, 303
Hauck B., North P., 1982, A&A, 114, 23
Hauck B., North P., 1993, A&A, 269, 403
Isobe S., Sasaki G., Norimoto Y., Takahashi J., 1986, PASJ, 38, 511
Jackisch G., 1972, AN, 294, 1
Kharitonov A.V., Tereshchenko V.M., Knyazeva L.N., 1988, Spectrophotometric Catalog of Stars, Nauka, Alma-Ata
King J.R., Villarreal A.R., Soderblom D.R., Gulliver A.F., Adelman S.J., 2003, AJ, 125, 1980
Kodaira K., 1973, A&A, 25, 93
Kurucz R.C., 1979, ApJS, 40, 1
Kurucz R.C., 1992, in "The Stellar Populations of Galaxies", IAU Symp. No, 149, eds. B. Barbuy, A. Renzini, Dordrecht, Kluwer, p. 225
Landstreet J.D., Barker P.K., Bohlender D.A., Jewison M.S., 1989, ApJ, 344, 876
Landstreet J.D., Bagnulo S., Andretta V., Fassati L., Mason E., Silaj J., Wade G.A., 2007, A&A, 470, 685
Leckrone D.S., Fowler, J.W., Adelman S.J.,1974, A&A, 32, 237
Molnar M.R., 1973, ApJ, 179, 527
Moon T.T., Dworetsky M.M., 1985, MNRAS, 217, 305
Musielok B., Madej J., 1988, A&A, 202,143
Muthsam H., Stępień K., 1980, A&A, 86, 240
Napiwotzki R., Schönberner D., Wenske V., 1993, A&A 268, 653
Paunzen E., Maitzen H.M., 1998, A&AS, 133, 1
Preston G.W., 1974, ARA&A, 12, 257
Pyper D.M., Adelman S.J., 1983, A&AS, 51, 365
Renson P., Gerbaldi M., Catalano F.A., 1991, A&AS, 89, 429
Rucinski S.M., Duerbeck H.W., 1997, PASP, 109,1340
Ryabchikova T., 2003, in "Magnetic fields in O, B and A stars: Origin and Connection to Pulsation, Rotation and Mass Loss" eds. L.A. Balona, H.F. Henrichs, R. Medupe, ASP Conf. Ser., vol. 305, 181
Schild R.E., Chaffee F., 1971, ApJ, 169, 529
Smalley B., Dworetsky M.M., 1993, A&A, 271, 515
Sokolov N.A., 1998, A&AS, 130, 215
Stępień K., 1968, ApJ, 154, 945
Stępień K., 1978, A&A, 70, 509
Stępień K., 1994, in "Chemically peculiar and magnetic stars", eds. J. Zverko, J. Ziznovsky, Tatranska Lomnica, Slovak Acad. of Sci., p. 8
Stępień K., Dominiczak R., 1989, A&A, 219, 197
Stępień K., Muthsam H., 1980, A&A, 92, 171
Stępień K., Muthsam H., 1987, A&A, 185, 225
Wolff S.C., 1967, ApJS, 15, 21